Pak. J. Bot., 54(4): 1335-1347, 2022. DOI: http://dx.doi.org/10.30848/PJB2022-4(24)

CLONING AND EXPRESSION ANALYSIS OF BNMYB90 AND BNMYB114 AND THEIR REGULATION ON *DFR* AND *F3H* IN *BRASSICA NAPUS*

ZHUANG LI[1#*], HAO LIANG[1#], XI JIANG[1], LIANGJUN HUANG[1], WEI ZHANG[1], SHI XING GUO[1], JIE LIU[1], WEIGUO LIU[2,3], KAI HOU[1], JUNBO DU[2,3], LILI LIN[4], JIN YANG[5,6], SHAO HONG FU[5,6] AND YONG CHENG WU[1*]

[1]*College of Agronomy, Sichuan Agricultural University, Chengdu 611130, China*
[2]*Institute of Ecological Agriculture, College of Agronomy, Sichuan Agricultural University, Chengdu 611130, China*
[3]*Key Laboratory of Crop Eco-physiology and Farming System in Southwest China, Ministry of Agriculture, Sichuan Agricultural University, Chengdu 611130, China*
[4]*College of Environmental Sciences, Sichuan Agricultural University, Chengdu 611130, China*
[5]*Crop Research Institute, Chengdu Academy of Agriculture and Forestry Sciences, Chengdu 611130, China*
[6]*Chengdu Branch of national rape Improvement Center, Sichuan, Chengdu 611130, China*
[#] *These authors Contributed equally to this work.*
**Corresponding authors' email:lizhuang2012@sicau.edu.cn; 445829036@qq.com*

Abstract

As one of the most important transcription factors, MYB75 and MYB90 are mainly regulators that influence pigment deposition by promoting the expression of genes through the anthocyanin synthesis pathway in Arabidopsis [*Arabidopsis thaliana* (L.) Heynh]. Yet the members of MYBs and the mechanism in modulation this process in oilseed rape (*Brassica napus* L.) is largely unknown. In this work, we found that two MYB TFs (BnMYB90 and BnMYB114) may influence anthocyanin biosynthesis. The transcription of *MYB90* and *MYB114* could be detected at all tested tissues in *B. napus*. Both BnMYB90 and BnMYB114 were located in the nucleus, which indicates they act as TFs and could modulate gene expression. Subsequently, results of both experiments *In vitro* and *In vivo* indicated MYBs bind to the promoters of *F3H* and *DFR*, which belong to an early and late gene of the anthocyanin biosynthesis pathway, respectively. Our experiments provide a preliminary and probable mechanism of how MYB TFs influence anthocyanin synthesis in oilseed rape.

Key words: *Brassica napus*; Expression analysis; Regulation; Function; Anthocyanin synthesis.

Abbreviations: bHLH, basic helix-loop-helix; CDS, coding sequence; DFR, dihydroflavonol-4-reductase; eGFP, enhanced green fluorescent protein;EMSA, electromobility shift assay; F3H1, flavonoid-3'-hydroxylase1; F3H2, flavonoid-3'-hydroxylase2; GFP, green fluorescent protein; MBS, MYB binding site; MBSI, MYB binding site 1; MBSII, MYB binding site 2; MYB, v-myb avian myeloblastosis viral oncogene homolog; PCR, polymerase chain reaction; qRT-PCR, quantitative real-time PCR; TF, transcription factor.

Introduction

As a secondary metabolite, anthocyanin widely exists in plants, especially in darker fruits and vegetables (Liu *et al*., 2018); and participates in the determination of flower color and fruit color (Albert *et al*., 2014; Fu *et al*., 2018; Francisco *et al*., 2013; Nishizaki *et al*., 2013; Sun *et al*., 2020; Wang *et al*., 2019). It also protects plants against harmful UV radition (Harborne & Williams, 2000; Solovchenko & Schmitz-Eiberger, 2003), and functions to oppose insect attacks and pathogen infection, even damage by herbivores (Harborne & Williams, 2000; Gould 2004; Golawska *et al*., 2014; Peters *et al*., 2002). Pigment deposition is affected by lots of factors, for instance, sucrose, light, temperature, drought, pathogens, wounds and plant hormones (Teng *et al*., 2005; Li *et al*., 2012; Xie *et al*., 2012; Jaakola, 2013; Mellway *et al*., 2009; Loreti *et al*., 2008; Qi *et al*., 2011).

Details study has been performed in higher plants, which revealed that anthocyanin is adjusted by the tryptophan aspartate dipeptide (WD)-repeat/bHLH/MYB complex (Espley *et al*., 2007; Xu *et al*., 2015). The R2R3-MYB transcription factors are a large family and 126 members have been found in Arabidopsis (Stracke *et al*., 2001; An *et al*., 2015). In maize, the first MYB transcription factor C1 was identified to regulate pigment deposition (Cone *et al*., 1986; Paz-Ares 1987). Several others related to flavonoid- adjusting MYB TFs were later characterized in different plants (Grotewold *et al*., 1991; Quattrocchio *et al*., 2006; Zhou *et al*., 2014; Kobayashi *et al*., 2004; Mathews *et al*., 2003). By binding directly to the promoters of structural genes, AtPAP1 and AtPAP2 influence the biosynthesis of anthocyanin in Arabidopsis (Gonzalez *et al*., 2010; Zuluaga *et al*., 2008).The purple color of tobacco plants could be generated by the overexpression of *AtPAP1* and *AtPAP2*, respectively (Borevitz *et al*., 2000). In apple, MdMYB1 not only responses to ethylene, but also modulates anthocyanin accumulation (An *et al*., 2018).

The research of pigment deposition in *B. napus* is lagging behind that in Arabidopsis. Recently, significant anthocyanin accumulation was found in the anthers after *OvPAP2* was transformed in *B. napus*. Red anthers and red petals could be found in overexpression XY35S: *OvPAP2* plants (Fu *et al*., 2018). Whole-genome re-sequencing and subsequently fine mapping suggested that a candidate gene *Bnpc1* associated with an orange petal trait was located in chromosome C9 of *B. napus* (Yao *et al*., 2017). Yet, the TFs that regulate anthocyanin accumulation in oilseed are rarely reported. In this study,

we focus on the mechanism of how BnMYB90 and BnMYB114 regulate *BnDFR* and *BnF3H*, which are respectfully regarded as the first key enzyme in the later period of anthocyanin biosynthesis pathway and a significant element of regulation pigment deposition in plants (Holton *et al*., 1995; Owens *et al*., 2011). We found that BnMYB90 and BnMYB114 are homologous to AtPAP1 and AtPAP2 in Arabidopsis. Subcellular localization analyses revealed that green fluorescent signals of BnMYB90 and BnMYB114 were observed in the nuclei. Mechanistic analyses showed that BnMYB90 and BnMYB114 may regulate anthocyanin accumulation partly through binding directly to *cis-acting* element of promoter of *BnDFR*, *BnF3H1* and *BnF3H2 In vivo* and *In vitro*. Taken together, these findings make some progress on the understanding the regulatory mechanisms of pigment accumulation in *B. napus*.

Materials and Methods

Materials: The oilseed rape seed was the Restorer line 18 (*B. napus*). To keep self-pollination, these plants were bagged upon entering the flowering period. Roots, stems, leaves, flowers and siliques were sampled, instantly frozen in liquid nitrogen, and then stored at -80°C for later analysis.

Phylogenetic tree: Protein sequences of MYB transcription factors of several species including Arabidopsis [*Arabidopsis thaliana*], grape (*Vitisvinifera*), maize (*Zea mays*), oilseed rape (*B. napus*) were aligned by software DNAMAN6.0. The neighbor-joining method was followed to construct the phylogenetic tree, and 1000 replicates were tested by bootstrap method. The bootstrap values are given next to each node. The phylogenetic analysis was performed using MEGA version 7.

RT-qPCR: Total RNA was isolated by Trizol (Invitrogen), and cDNA synthesis was done using the Fast King RT Kit (Tiangen). For Real-time qRT-PCR, 10 µl of cDNA was diluted to 200 µl, then 1 µl was used for following experiment. The reaction was performed by SYBR Green MasterMix (Takara). Relative quantification of mRNA was calculated using the $2^{-\Delta\Delta Ct}$ method. All of the primers used in this study are shown in the supplemental table 3 (Supplemental Table 3). The *BnActin*gene was used as the external control. The experiments were done at least three times.

Subcellular localization analysis: CDSs of *BnDFR*, *BnF3H1*, *BnF3H2*, *BnMYB90* and *BnMYB114* were cloned into pCAMBIA2300-35S-eGFP to generate Pro35S: BnDFR-eGFP, Pro35S:BnF3H1-eGFP, Pro35S: BnF3H2-eGFP, Pro35S: BnMYB90-eGFP and Pro35S: BnMYB114-eGFP, respectively. The plasmid pCAMBIA2300-35S-eGFP (Pro35S: eGFP) expressing eGFP protein alone, was used as the control. These constructs were transiently transformed into onion epidermal cells by biolistic bombardment using standard procedures. After bombardment, epidermal peels were incubated at 28°C for 24 h in the adrk. The subcellular localization of the fused proteins was visualized by laser scanning confocal microscope (Nikon).

Yeast one-hybrid assays: The coding sequences of *BnMYB90* and *BnMYB114* were inserted into the pGADT7-Rec2 vector (Clontech), and the promoter fragments of *BnDFR*, *BnF3H1* and *BnF3H2* were cloned into the pHIS2 vector (Clontech). The co-transformed Y2H Gold yeast strains were plated on –Trp/-Leu/-His medium, 3-amino-1, 2, 4-triazole was supplied an appropriate concentration.

Electromobility shift assays: The CDSs of *BnMYB90* and *BnMYB114* were inserted into the PET28a (+) vector to generate recombined vectors. Then the fusion proteins of BnMYB90 and BnMYB114 and biotin-labeled probes (*BnDFR* probe, *BnF3H1* probe and *BnF3H2* probe) (Viagene Biotech Inc, Changzhou, China) were used. The unlabeled or mutant probes were used as competitors. The Gata1 by biotin-labeled probe was used as control in conventional EMSA. The vector protein was used as controls in competitor EMSA and mutant EMSA. Conventional probe sequences in *BnDFR*, *BnF3H1* and *BnF3H2* promoter and Gata1 control probe sequence for EMSA are shown in the supplemental table 1 (Supplemental Table 1). Mutant probe sequences in *BnDFR*, *BnF3H1* and *BnF3H2* promoter for EMSA are shown in the supplemental table 2 (Supplemental Table 2). The EMSAs were performed by non-radioactive EMSA Kits (ThermoFisher Scientific, USA) according to the manufacture's instruction.

Supplemental Table 1. Conventional probe sequences in *BnDFR*, *BnF3H1* and *BnF3H2* promoter and Gata1 control probe sequence for EMSA.

Promoter	Original probe sequences
BnDFR	CAAGTCCTTAGCCAACTAACGTTCCACACG
BnF3H1	CTAGATTAGAGTATAACTGACCACGTTCTG
BnF3H2	CTCAAATTCACCCAACATGACATAACTT
Gata1	CACTTGATAACAGAAAGTGATAACTCT

Supplemental Table 2. Mutant probe sequencesin*BnDFR*, *BnF3H1* and *BnF3H2* promoter for EMSA.

Promoter	Mutant probe sequences
BnDFR	CAAGTCCTTAGCCGACGAACGTTCCACACG
BnF3H1	CTAGATTAGAGTATGCCGGACCACGTTCTG
BnF3H2	CTCAAATTCACCCGAGATGACATAACTT

Dual luciferase assays: The reporters were generated by recombining *BnDFR, BnF3H1* and *BnF3H2* truncation fragments into pGreenII 0800-LUC vector, respectively. Full-length *BnMYB90* and *BnMYB114* were inserted into pGreenII 62-SK vector to generate the effectors, respectively. The recombinant vectors were transformed into Agrobacterium strain GV3101. Tobacco leaves were infected with the mixed Agrobacterium strains. LUC/REN activity was examined by a GloMax multi-functional detector (Promega, USA).

Supplemental Table 3. List of primers used in this study.

Primer	Primer sequence	Tm	Number of cycle	Amplification size	Vector	Purpose
BnF3H1-F	ATGGCTCCAGGAACTCTAAC	58℃	35	1076	P-EASY-Simple-T	Gene Clone
BnF3H1-R	CTAAGCGATGATTTGGTC					
BnF3H2-F	ATGGCTCCAGGAACTCT	58℃	35	1076		
BnF3H2-R	CTAAGCGATGATTTGGTCTAG					
BnDFR-F	ATGGTAGCTCACAAAGAGAC	58℃	35	1157		
BnDFR-R	CTAAGCACAGATCTGCTG					
BnMYB90-F	ATGGAGGATTCGTCCAAAGG	58℃	35	752		
BnMYB90-R	CGCGCTAATCAAGTTCTACAG					
BnMYB114-F	ATGGAGGGTTCGTC	58℃	35	323		
BnMYB114-R	CTCACTAATGGGTGTTCCAG					
q-BnMYB90-F	CAGGTGGTCTTTAATTGCTGG	60℃	40	250		qRT-PCR
q-BnMYB90-R	CATGGAGGAACAACGTCAAC					
q-BnMYB114-F	GTATGGAGAAGGGAAATGGC	60℃	40	210		
q-BnMYB114-R	GGTCCGACCGGGTAATCTA					
q-BnACTIN-F	TGCTCTTCCTCACGCTATCCTC	60℃	40	215		
q-BnACTIN-R	GCTCGTAGTTCTTCTCCACCG					
BnF3H1-F1	CGACTCACTATAGGGCGAATT CGGCACTGCCTTGCACGGTT	60℃	35	1073	pCAMBIA 2300-35S-eGFP	Subcellular localization
BnF3H1-R1	AGCCTCTAGACCAAATCATCGC TGTCGACACTAGTACCATGGTGA					
BnF3H2-F1	ATGGTCTGGAGGATCCTCTAGAA TGGCTCCAGGAACTCTAACTG	60℃	35	1073		
BnF3H2-R1	AGCCTCTAGACCAAATCATCGCT GTCGACACTAGTACCATGGTGA					
BnDFR-F1	ATGGTCTGGAGGATCCTCTAGA ATGGTAGCTCACAAAGAGACCG	60℃	35	1154		
BnDFR-R1	CGGCACAGCAGATCTGTGCTGT CGACACTAGTACCATGGTGA					
BnMYB90-F1	GGACAGGGTACCCGGGGATTC ATGGAGGATTCGTCCAAAGG	60℃	35	749		
BnMYB90-R1	GATGGAGAGACTGTAGAACT TGATTCTAGAATGGGTGTTCCAGTAA TTTTGACG					
BnMYB114-F1	GGACAGGGTACCCGGGGAT TCATGGAGGATTCGTCCAAAGGG	60℃	35	320		
BnMYB114-R1	GTCAAAAATTACTGGAACA CCCATTCTAGAATGGGTGTT CCAGTAATTTTGACG					
Pro-BnF3H1-F1	CGACTCACTATAGGGCGAAT TCACGGTTGGTTGTTATTGCT	62℃	35	1975	pHIS2	Y1H
Pro-BnF3H1-R1	GCTTCAATCGCCCTATAGAT TTCCGAGCTCAAGAGAAA GAGAGTGCGTGG					
Pro-BnF3H2-F1	CGACTCACTATAGGGCGAA TTCTTCTCTACGAAAAGCCAAG	62℃	35	1685		
Pro-BnF3H2-R1	CCAACACAAAGGGCAGCT GGGAGCTC GTGTTGGTTCGGTTGTGTAAG					
Pro-BnDFR-F1	CGACTCACTATAGGGCGAA TTCGCGTTCATTTGATAAA GAGGTAGC	62℃	35	1722		
Pro-BnDFR-R1	GAAGATTTCCACCGAAGA AGGGAGCTCCTTCGGTGG AAATCTTCGTGC					
BnMYB90-F2	CGTACCAGATTACGTCCA TATGATGGAG GATT	60℃	35	752	pGADT7-Rec2	
BnMYB90-R2	CGTCCAAAGG TGGAGAGACTGTAGAAC TTGATGAATTCCTAATCAA GTTCTACAGTC					
BnMYB114-F2	CGTACCAGATTACGTCCA TATGATGGAGGGTTCGT	60℃	35	323		
BnMYB114-R2	CCAAAGG TGGAGAGACTGTAGAA CTTGATGAATTCCTAA TGGGTGTTCCAG					

Supplemental Table 3. List of primers used in this study.

Primer	Primer sequence	Tm	Number of cycle	Amplification size	Vector	Purpose
BnMYB90-F3	GGACAGGGTACCCGGGGCGGCCGCATGGAGGATTCGTCCAAAGGG	60℃	35	749	PET-28a (+)	EMSA assays
BnMYB90-R3	GGTACTAGTGTCGACCTCGAGATCAAGTTCTACAGTCTCTCCATCCA					
BnMYB114-F3	GGACAGGGTACCCGGGGCGGCCGCATGGAGGGTTCGTCCAAAGG	60℃	35	320		
BnMYB114-R3	GGTACTAGTGTCGACCTCGAGATGGGTGTTCCAGTAATTTTTGACG					
p-BnDFR-F3	ACGACTCACTATAGGGCGAATTGGGTACCTAAATAAGATAG	60℃	35	436		
p-BnDFR-R3	CGGGCTGCAGGAATTCGATATCAAGCTTCTTCTTCGGTGG					
p-BnDFR-m-F3	ACGACTCACTATAGGGCGAATTGGGTACCTAAATAAGATAG	60℃	35	436		
p-BnDFR-m-R3	CGGGCTGCAGGAATTCGATATCAAGCTTCTTCTTCGGTGG					
p-BnF3H1-F3	ACGACTCACTATAGGGCGAATTGGGTACCGGCACTGCCTTGCACG	60℃	35	436		
p-BnF3H1-R3	CGGGCTGCAGGAATTCGATATCAAGCTTC					
p-BnF3H1-m-F3	AAGTGTAAATCTGGTGACGACTCACTATAGGGCGAATTGGGTAC	60℃	35	436	PGreenII 0800-LUC	Dual Luciferase assays
p-BnF3H1-m-R3	CGGCACTGCCTTGCACCGGGCTGCAGGAATTCGATATCAAG					
p-BnF3H2-F3	CTTCAAGTGTAAATCTGGTGACGACTCACTATAGGGCGAATTGGGTA	60℃	35	448		
p-BnF3H2-R3	CCGACCCGAACCGCGGGCTGCAGGAATTCGATATCAAGCTT					
p-BnF3H2-m-F3	CAGCTGCCCTTTGTGTTGACGACTCACTATAGGGCGAATTGGGTAC	60℃	35	448		
p-BnF3H2-m-R3	CGACCCGAACCGCGGGCTGCAGGAATTCGATATCAAGCTTCAGCTGCCCTTTGTGTTG					
BnMYB90-F4	GCTCTAGAACTAGTGGATCCCCCGGGATGGAGGATTCGTCCAAAGG	60℃	35	752	PGreenII 62-SK	
BnMYB90-R4	CTCGAGGTCGACGGTATCGATAAGCTTCTAATCAAGTTCTACAGTCTCTCCAT					
BnMYB114-F4	GCTCTAGAACTAGTGGATCCCCCGGGATGGAGGGTTCGTCCAAAGG	60℃	35	323		
BnMYB114-R4	CTCGAGGTCGACGGTATCGATAAGCTTCTAATGGGTGTTCCAGTAATTTTTG					

Statistical data analysis

The obtained data were analyzed via one-way ANOVA; letters indicate statistical differences ($p<0.05$).

Results

Identification of MYB genes in oilseed rape: MYB75 (PAP1) and MYB90 (PAP2) are mainly regulators for biosynthesis of anthocyanin in Arabidopsis. Two R2R3 MYB genes, *BnMYB90* and *BnMYB114*, were isolated because of their higher homology to AtMYB75 or AtMYB90 (Supplemental Fig. 1). The results of sequencing analysis indicated that BnMYB90 and BnMYB114 were localized on chromosome 7 and chromosome 2 in C class, respectively (Supplemental Fig. 2).

Predicted coding protein sequence alignment results showed that intact R2 domain and imperfect R3 domain were included in both BnMYB90 and BnMYB114. In addition, only an intact [DE]Lx2[RK]x3Lx6Lx3R element is included in BnMYB114 (Fig. 1a), which is important for interaction with bHLH proteins (Zimmermann *et al*., 2004). The relationship analyses of BnMYB90 and BnMYB114 to other MYB TFs regulated flavonoid metabolism in other species was analyzed by constructing the phylogenetic tree. The results indicated that BnMYB90 and BnMYB114 proteins are highly homologous with AtPAP1 and AtPAP2, respectively, which verify the results of supplemental Fig. 1 (Fig. 1b).

Gene expression analysis: RT-qPCR of *BnMYB90* and *BnMYB114* were performed by a CFX96 Real-Time PCR detection system (Bio-Rad). The results showed that expression of *BnMYB90* and *BnMYB114* are different across plant tissues. The *BnMYB90* expression level was the highest in roots and was the lowest in siliques at 27 d after pollination. In addition, the *BnMYB114* transcript level was the highest in siliques at 35 d after pollination, but was the lowest in stems (Fig. 2).

Subcellular localization of BnMYBs, BnDFR and BnF3H: In general, TFs localized in nucleus or/and cytoplasm to adjust expression of downstream genes. To test the distribution of BnMYB90 and BnMYB114 in the plant cell, subcellular localization assays were performed. The green fluorescence was well-distributed in the transformed cell when the empty green fluorescent protein (GFP) was expressed. The BnMYB90-eGFP and BnMYB114-eGFP accumulated at the nucleus of onion epidermal cells (Fig. 3e-f). These predicted proteins in oilseed rape were of higher homology to AtPAP1 or AtPAP2 which suggests that they play a crucial role in anthocyanin pigment biosynthesis pathway. To test this possibility, subcellular localization of BnF3H and BnDFR were also performed, which are recognized as early and late genes in the anthocyanin biosynthesis pathway, respectively. When the BnDFR-eGFP, BnF3H1-eGFP and BnF3H2-eGFP fusion proteins were transiently expressed in the onion epidermal cells, green fluorescent signals were found in the whole cell including nuclei (Fig. 3b-d).

Yeast one-hybrid assay: We confirmed a direct interaction of BnMYB90 and BnMYB114 with upstream regions of *BnDFR*, *BnF3H1* and *BnF3H2* by a yeast one-hybrid system. The upstream fragments of *BnDFR*, *BnF3H1* and *BnF3H2* were inserted into the pHIS2 vector, respectively, and the full length CDSs of *BnMYB90* and *BnMYB114* were subcloned into the pGADT7-Rec2 vector, respectively. The experiments used 3-amino-1,2,4-triazole (50 mM) to reduce the background signal. The results indicated that in the presence of BnMYB90-AD, both *BnDFR: HIS2*, *BnF3H1:HIS2* and *BnF3H2:HIS2* were activated, as showed by colony growth on three deficiency culture medium. In contrast, no growth was observed with the HIS2 empty vector. Similar results were also observed in BnMYB114-AD (Fig. 4).

BnMYBs bind specifically to the BnDFR/ BnF3H1/ BnF3H2 promoters: To assess possible cis-acting elements, promoter sequences of *BnDFR*, *BnF3H1* and *BnF3H2* genes were analyzed using PlantCARE software, respectively. The results indicated that the MBSI or MBSI-like sequences were found in the *BnF3H1*, *BnF3H2* and *BnDFR* promoter. And the MBSII sequences were found in all three gene promoters (Supplemental Fig. 3). PlantCARE software analysis results also showed that different numbers of putative G-box and G-box-related hexamers were contained in the promoter sequence of *BnDFR*/ *BnF3H1*/*BnF3H2*. In addition, there were also multiple elements that respond to other biological stresses and abiotic stresses in the promoter sequence of three genes (data not shown).

To verify whether BnMYB90 and BnMYB114 were bound to sites MBSI or/and MBSII in the *BnDFR*, *BnF3H1* and *BnF3H2* promoters, conventional EMSA assays were carried out. The results indicated that BnMYB90 and BnMYB114 bind to the MBSII of the *BnDFR* promoter, to MBSI of the *BnF3H1* promoter, and to MBSII of the *BnF3H2* promoter, respectively (Supplemental Fig. 4b-c). When more competitive probes were added, the binding signal became weaker. However, the binding signals were negligibly affected when mutated probes were added (Fig. 5). These results indicated that both BnMYB90 and BnMYB114 bound to fragments of the upstream regions of*BnDFR*, *BnF3H1* and *BnF3H2 In vitro*.

Transient dual luciferase assay: To verify whether BnMYB90 and BnMYB114 activate or inhibit to *BnDFR*, *BnF3H1* and *BnF3H2 In vivo*, transient dual luciferase assays were done in *Nicotiana.benthamiana* L. leaves. The full length CDSs of *BnMYB90* and *BnMYB114* were inserted into the pGreenII 62-SK vector to construct effectors, and the fragments of upstream regions of *BnDFR*, *BnF3H1* and *BnF3H2* or the mutated fragments of *BnDFR*, *BnF3H1* and *BnF3H2* were subcloned into the pGreenII 0800-LUC vector to construct reporters (*BnDFR*pro: LUC, *BnF3H1*pro: LUC and *BnF3H2*pro: LUC, or *BnDFR*pro-m: LUC, *BnF3H1*pro-m: LUC and *BnF3H2*pro-m: LUC, respectively). Transformed *Agrobacterium tumefaciens* GV3101 were co-inserted into *N. benthamiana* leaves. The results showed the co-transformation of 35Spro: BnMYB90 with *BnDFR*pro/*BnF3H1*pro/*BnF3H2*pro: LUC resulted in a higher LUC to REN ratio. Similar results were also detected in co-transformation of 35Spro: BnMYB114 with *BnDFR*pro/ *BnF3H1*pro/ *BnF3H2*pro: LUC, while co-transformation of 35Spro: BnMYB90 with *BnDFR*pro-m/*BnF3H1*pro-m/*BnF3H2*pro-m: LUC resulted in a weak luminescence signal. Similar results were also detected in co-transformation of 35Spro: BnMYB114 with *BnDFR*pro-m/*BnF3H1*pro-m/*BnF3H2*pro-m: LUC (Fig. 6).

Sequences producing significant alignments Download Manage Columns Show 100

Description	Max Score	Total Score	Query Cover	E value	Per. Ident	Accession
Arabidopsis thaliana putative transcription factor (MYB75) mRNA, complete cds	1373	1373	100%	0.0	99.87%	AF062908.1
Arabidopsis thaliana myb domain protein 90 (MYB90), mRNA	734	734	100%	0.0	84.44%	NM_105310.4
Brassica napus MYB transcription factor 90 (MYB90.1) mRNA, complete cds	518	518	100%	2e-142	79.71%	KF738284.1
PREDICTED: Brassica napus transcription factor MYB114 (LOC106394969), mRNA	556	556	99%	4e-154	80.35%	XM_013835513.2

Supplemental Fig. 1. Sequence alignment of *BnMYB90* and *BnMYB114* with *AtMYB75* and *AtMYB90*.

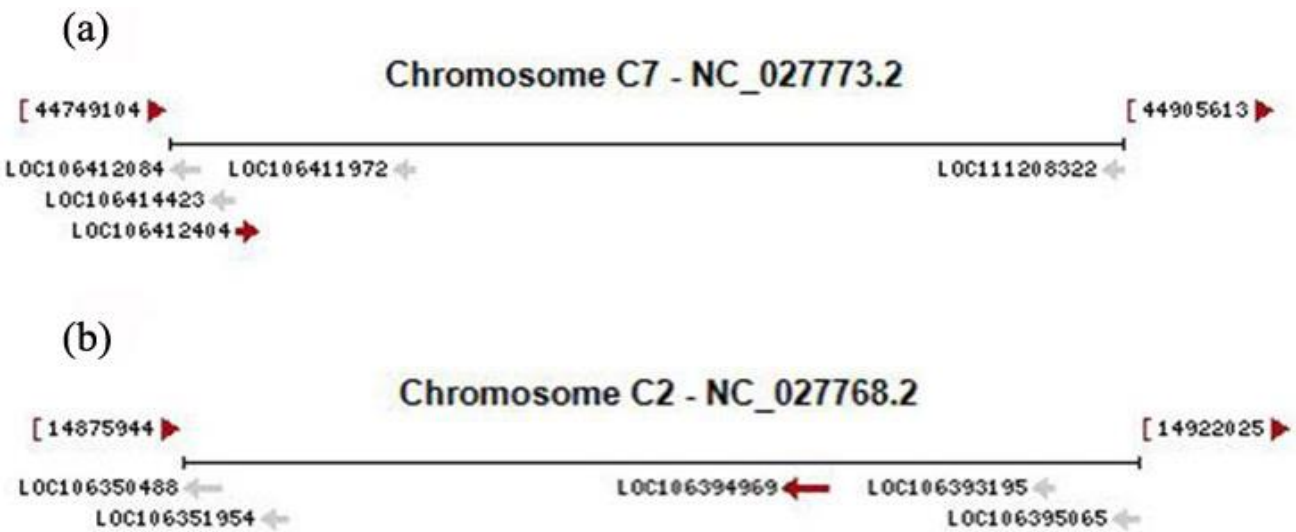

Supplemental Fig. 2. Position of *BnMYB90* and *BnMYB114* on chromosome in *Brassica napus*. (a) *BnMYB90* locates in chromosome C7, and (b) *BnMYB114* locates in chromosome C2.

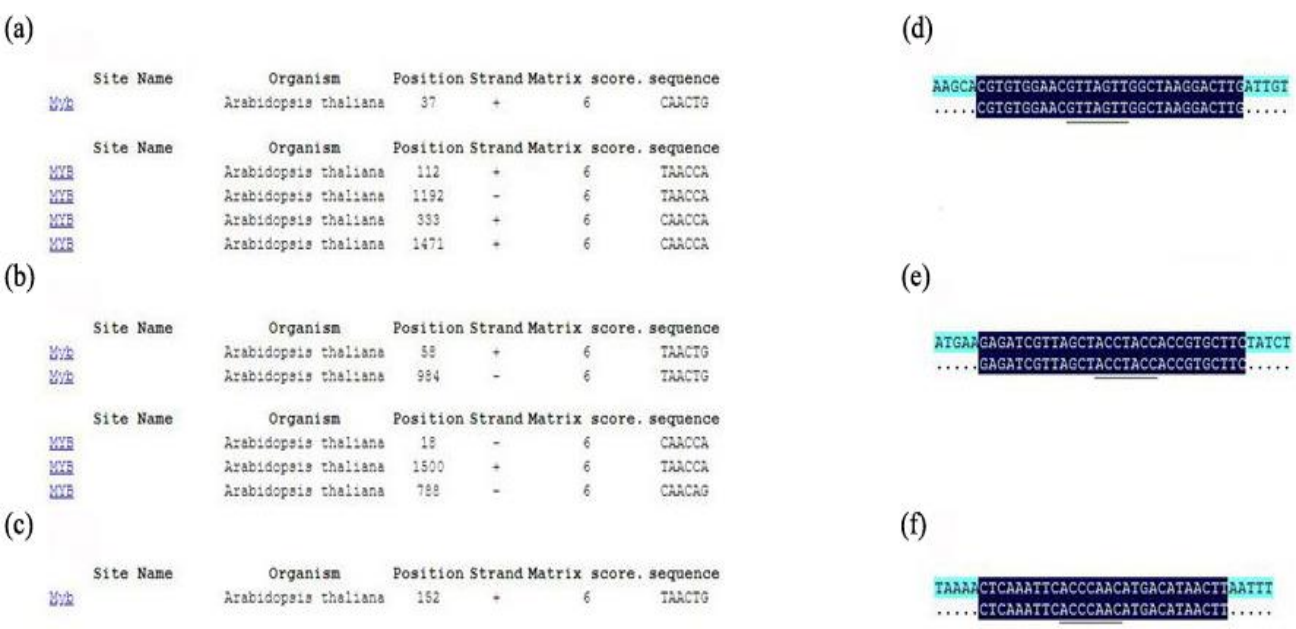

Supplemental Fig. 3. Prediction MBSI, MBSI-like and MBSII in the promoter sequence of *BnDFR*, *BnF3H1* and *BnF3H2*. (a) Prediction MBSI and MBSI-like is in the promoter sequence of *BnDFR*. (b) Prediction MBSI and MBSI-like is in the promoter sequence of *BnF3H1*. (c) Prediction MBSI is in the promoter sequence of *BnF3H2*. (d) Alignment the sequence including in MBSII with the promoter sequence of *BnDFR*. (e) Alignment the sequence including in MBSII with the promoter sequence of *BnF3H1*. (f) Alignment the sequence including in MBSII with the promoter sequence of *BnF3H2*. The single black line under the sequence bottom represents MBSII motif in promoter sequence of *BnDFR*, *BnF3H1* and *BnF3H2*, respectively.

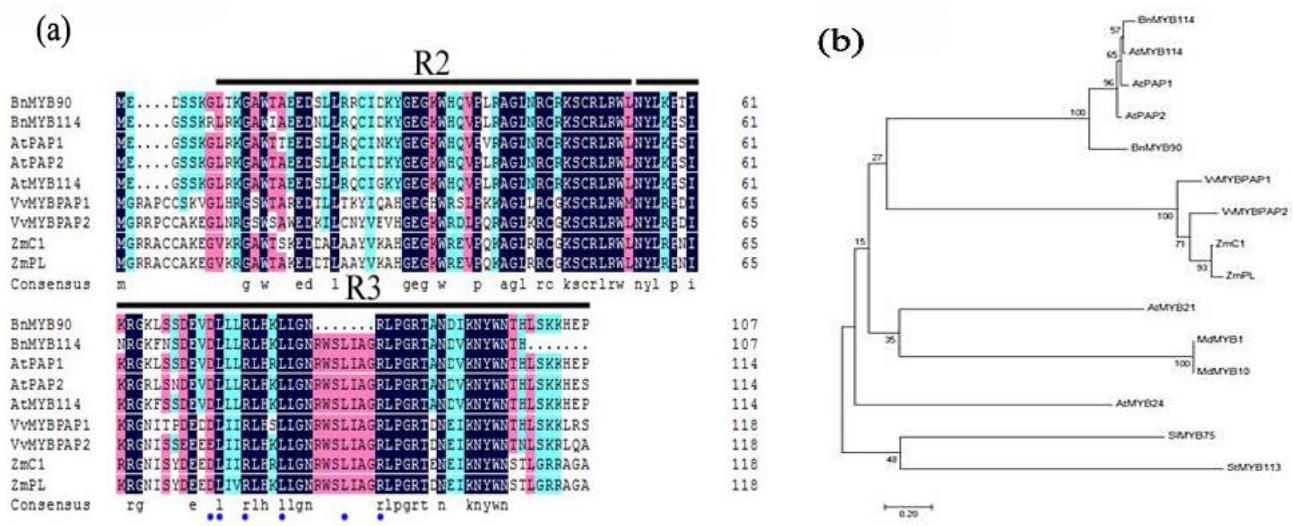

Fig. 1. Characterization of flavonoid regulatory BnMYBs in oilseed rape. Multiple alignment analysis of BnMYB90 and BnMYB114 proteins and other MYBs in various species was performed using DNAMAN 6.0. (a). Blue dots indicate the residues took part in the interaction with the bHLH. The R2 and R3 replications in the MYB domain are showed by black bar. (b). Phylogenetic tree of BnMYB proteins and other MYBs based on protein sequences with SlMYB75 from tomato (*Solanum lycopersicum* L.) and StMYB113 from potato (*Solanum tuberosum* L.) as outgroup.

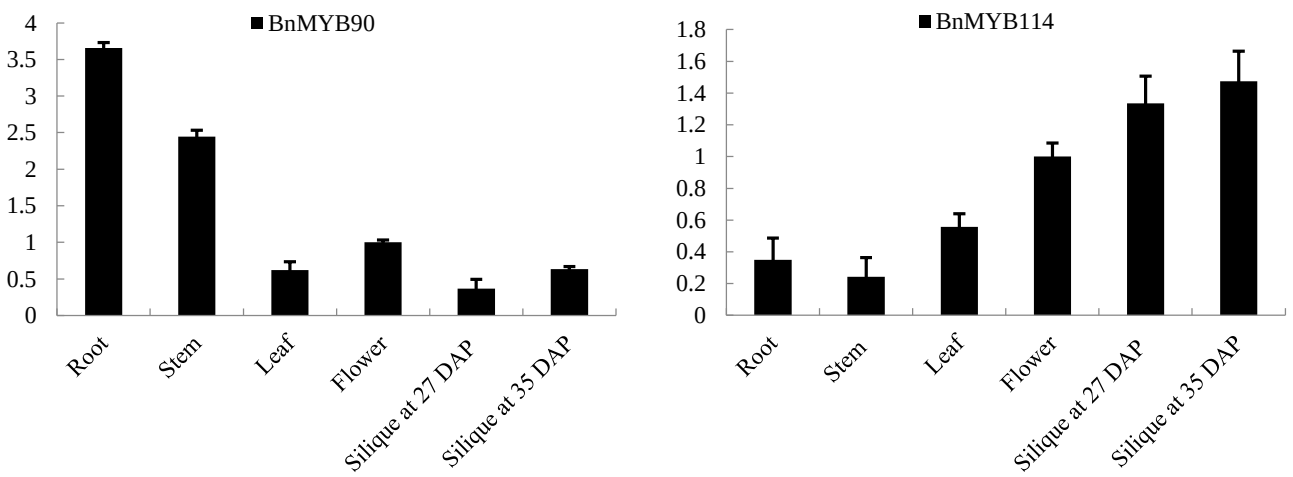

Fig. 2. (a) and (b) Expression analysis of *BnMYB90BnMYB114* in various of tissues. RT-qPCR was done with three biological replicates. Data shows the means of three independent experiments. Dissimilar letters represent significant differences by one-way ANOVA and Tukeyposthoc test (p<0.05).

Discussion

Anthocyanin biosynthesis genes are tightly regulated through TFs. A sequence alignment result showed that not BnMYB90 but BnMYB114 contained intact [DE] Lx_2 [RK] x_3 Lx_6 Lx_3 R motif (Fig. 1a), which is considered as a significant element to interact with bHLH proteins (Zimmermann *et al*., 2004). BnMYB90 included in an incomplete but conserved motif to suggest that its interaction with bHLH TF became weaker even from indirect interaction. The WD-repeat/bHLH/MYB complex which modulates anthocyanin pigment accumulation were shown for various species (Li *et al*., 2019; Tao *et al*., 2020; Montefiori *et al*., 2015; Chagne *et al*., 2013; Jin *et al*., 2016). While the conservative motif appeared differently between BnMYB90 and BnMYB114, which suggested different MYB TFs may play an important role in pigment deposition by forming a complex with different TF family members in oilseed rape. Phylogenetic analysis result showed that BnMYB90 and BnMYB114 are highly homologous with AtPAP1 and AtPAP2 (Fig. 1b), which suggested functional conservation and homology of *MYB* genes between Arabidopsis and oilseed rape.

To analyze the expression level of *BnMYB90* and *BnMYB114*, root, stem, leaf, flower and silique at different time after pollination were collected and analyzed by qRT-PCR. Our result indicated that *BnMYB90* and *BnMYB114* were expressed in all tested tissues of *Brassica napus*. The highest expression levels of *BnMYB90* were in below-ground tissues, followed by stems and flowers of the aerial tissues. However, excluding stems, a clearly higher expression level of *BnMYB114* was detected in aerial parts than in roots. The highest expression level of *BnMYB114* was in siliques at 35 d after pollination, although this was no obvious divergence from that in siliques at 27 d after pollination. The expression level of *BnMYB114* in flowers was lower than that in siliques after different pollination times (Fig. 2). Jasmonate (JA) is a vital hormone that

regulates many aspects of plant growth including root growth (Stintzi and Browse 2000; Xiao *et al*., 2004; Yoshida *et al*., 2009). The root stem cell niche patterning is adjusted by the TFs, which is a auxin-inducible PLT gene (Aida *et al*., 2004; Galinha *et al*., 2007). Strigolactones are a large class of different signaling compounds, which regulates many aspects of plant development including root growth (Snowden *et al*., 2005). Brassinosteroids regulate the expression of BRL3, with transcription regulated by BES1in different subsets of cells of the root apex (Salazar-Henao *et al*., 2016). The high expression level of *BnMYB90* detected in roots suggested the exclusion of synthesis of anthocyanin, it may be involved in multiple hormone signaling pathways. An increased polyunsaturated fatty acid content in yeast and Arabidopsis seeds was observed through expression of two PDCTs derived from flax (*Linum usitatissimum*) (Wickramarathna *et al*., 2015). The *FAD* gene family consists of many members, among these some were shown as modulating fatty acid synthesis and metabolism. By artificially inducing *fad2* gene mutation, the content of linoleic acid in sunflower seed oil was inhibited and the content of oleic acid was significantly increased (Miller *et al*., 1987). By heterologous expression of 35S:*NtFAD3* in rice, stable transgenic rice was obtained with α-Linolenic acid content that increased up to 2.5-fold when compared with the control (Shimada *et al*., 2010). The expressions of *FAD2* and *FAD6* are found in different organs (Hatzopoulos *et al*., 2002; Banilas *et al*., 2005). The *FAD7* gene is responsible for the ω-3 fatty acid desaturase, which is triggers the production of trienoic fatty acids. As one of the trienoic fatty acid family members, linolenic acid was detected in seeds. The little modified transcript levels of *GmFAD7-1*, *GmFAD7-2* and *GmFAD8* were found in developing seeds (Andreu *et al*., 2010). Lysophosphatidic acid acyltransferase catalyzes the second fatty acid to produce phosphatidic acid, which is regarded as a link to lysophosphatidic acid and consisted of at least nine members in Arabidopsis (Roscoe, 2005). Excluding *AtLPAT3*, the expressions of *AtLPAT2*, *AtLPAT4* and *AtLPAT5* were demonstrated in siliques (Kim *et al*., 2005). The expression pattern of *KCS* family was detected in Arabidopsis, which indicated that most family members express in siliques (Joubes *et al*., 2008). In Arabidopsis, two homologous genes are found with the yeast *KCR* gene, and expressions were demonstrated in various tissues including siliques (Beaudoin, 2009). The time frame of 20 to 35 d after pollination is not only the key period of oilseed rape yield formation (Liu *et al*., 2016), but this is also the key period for oilseed rape fat accumulation and fatty acid transformation. The high expression level of *BnMYB114* was detected in the aerial parts especially in siliques after different pollination times; this suggested that the transcription factor may intervene fatty acid synthesis and metabolism by adjusting the expression of key genes.

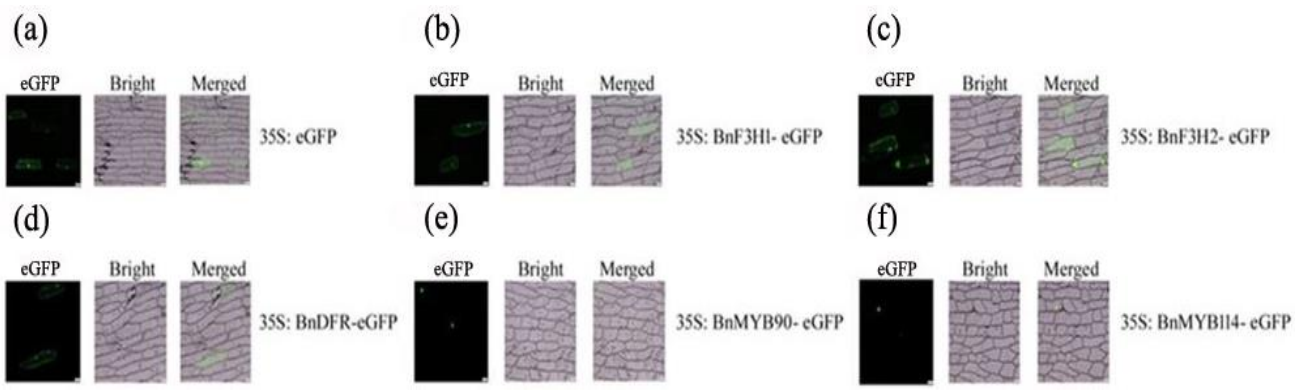

Fig. 3. (b), (c), (d), (e) and (f) Subcellular localization of BnF3H1-eGFP, BnF3H2-eGFP, BnDFR -eGFP, BnMYB90-eGFP, BnMYB114-eGFP in the onion epidermal cells. (a). pCAMBIA2300-35S-eGFP was used as a control. Bars = 50 μm.eGFP, enhanced green fluorescent protein.

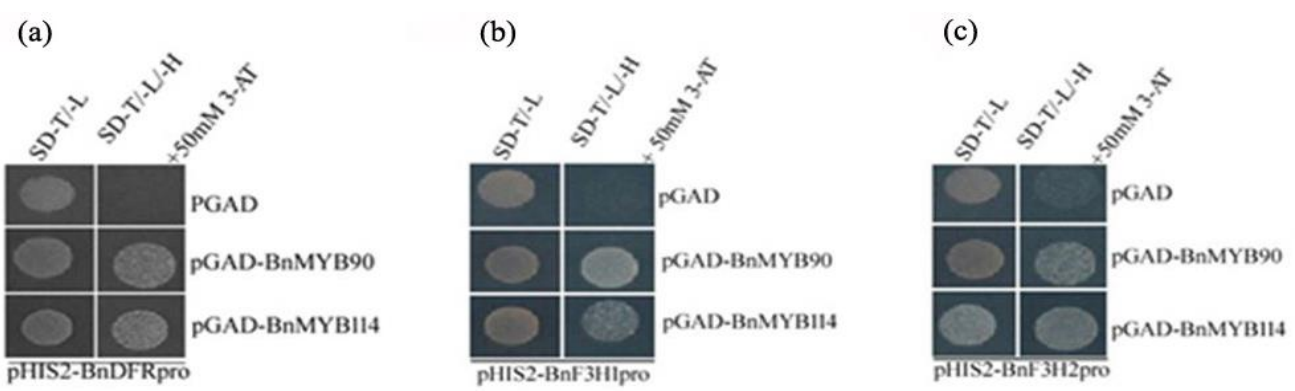

Fig. 4. (a), (b) and (c)Y1H assays indicate BnMYB90 and BnMYB114 interaction with the promoters of *BnDFR*, *BnF3H1* and *BnF3H2*, respectively. The promoter of *BnDFR*, *BnF3H1BnF3H2* and were inserted into the pHIS2 vectors, and the *BnMYB90* and *BnMYB114* genes were cloned into the pGADT7 vector, respectively. (a), (b) and (c) The columns represent the addition of the pHIS2-$BnDFR_{pro}$ vector, pHIS2-$BnF3H1_{pro}$ vector and pHIS2-$BnF3H2_{pro}$ vector, respectively. The rows indicate the addition of the pGADT7-Rec2 and pGADT7-BnMYB90 vectors or the pGADT7-Rec2 and pGADT7-BnMYB114 vectors, respectively.

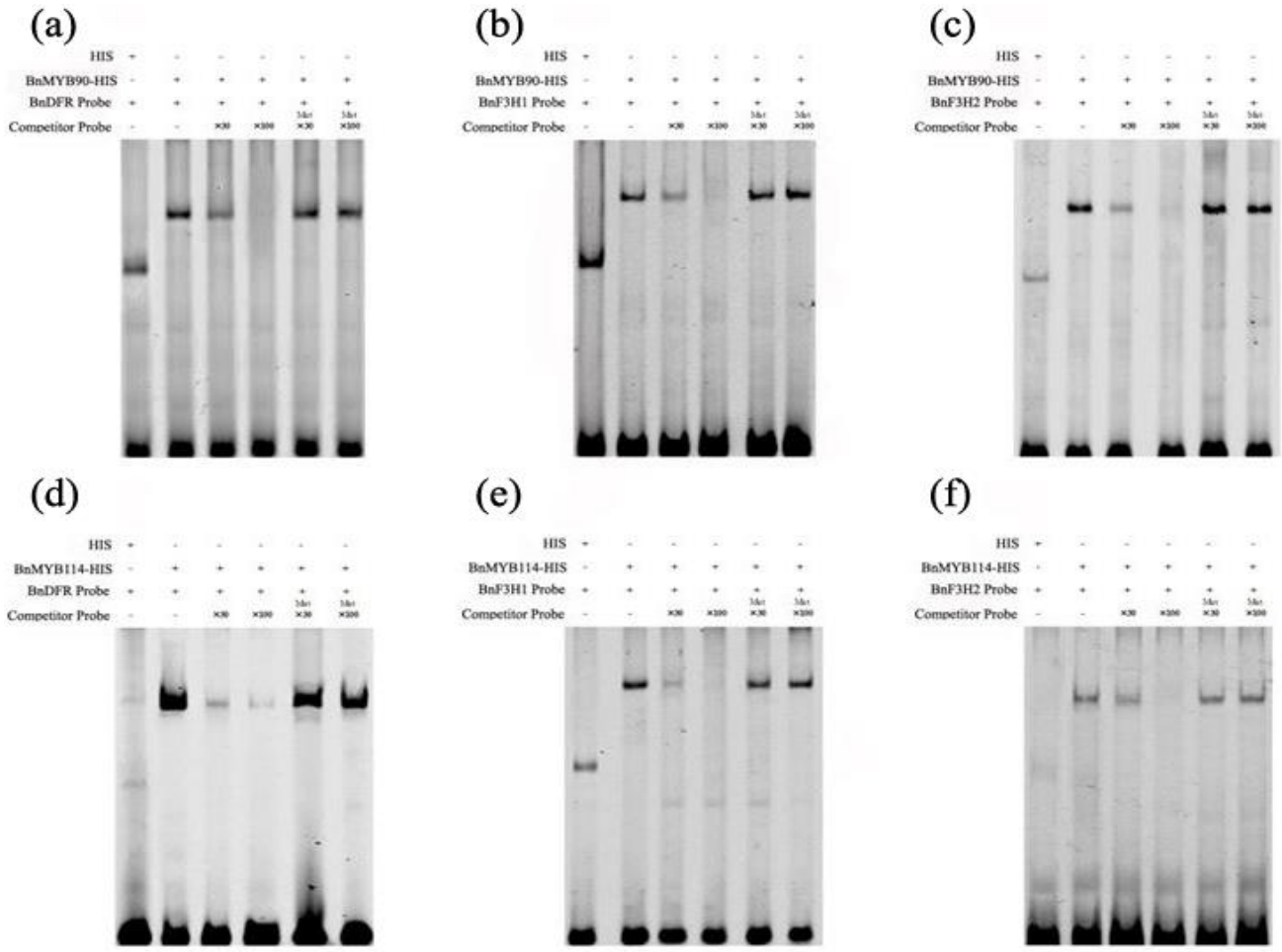

Fig. 5. (a), (b) and (c) EMSA indicate the binding of BnMYB90-HIS to the *BnDFR*, *BnF3H1* and *BnF3H2* promoters; (d), (e) and (f) EMSA indicate the binding of BnMYB114-HIS to the *BnDFR*, *BnF3H1* and *BnF3H2* promoters. HIS alone was used as negative control. Adding excess (30-fold and 100-fold) of unlabeled probes or mutated probes were used to induce competition. The probe sequences are illustrated in supplemental tables 1 and 2.

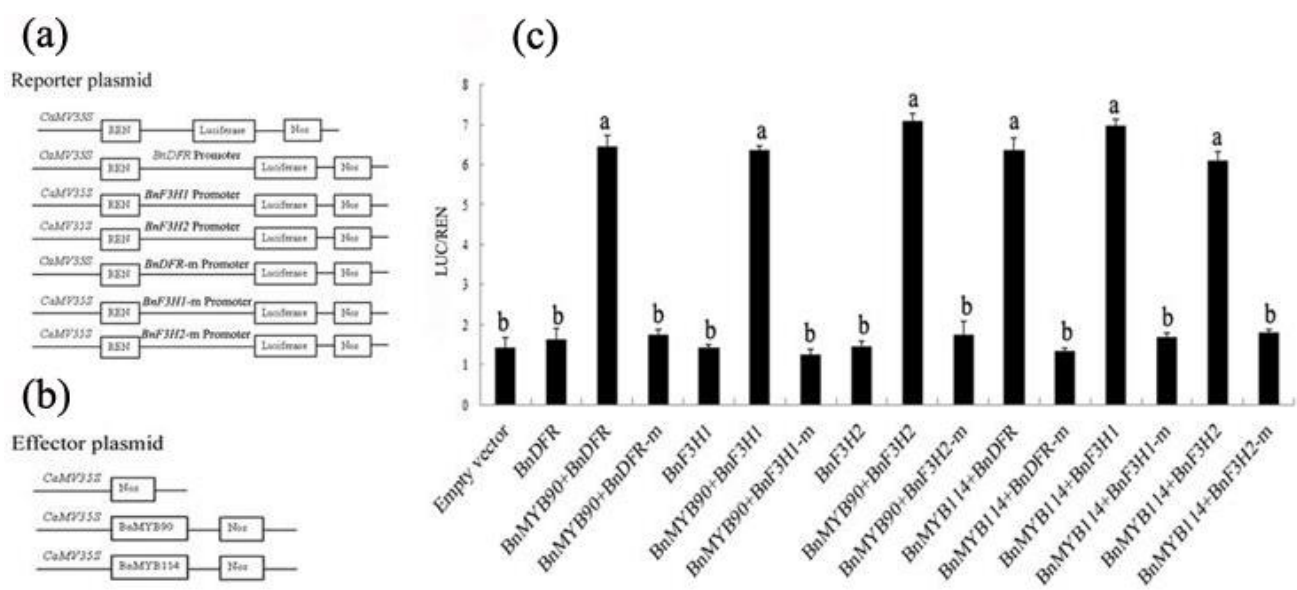

Fig. 6. BnMYB90 and BnMYB114 activate directly the transcription of *BnDFR*, *BnF3H1*, *BnF3H2*. (a) and (b) Illustrative diagram of the reporter vectors and Illustrative diagram of the effector vectors. The promoter fragment of *BnDFR*, *BnF3H1*, *BnF3H2* and or the mutated promoter fragment of *BnDFR*, *BnF3H1*, *BnF3H2* were inserted into the pGreenII 0800-LUC plasmid to produce the reporter constructs, respectively. The *BnMYB90* and *BnMYB114* genes sub-cloned into the pGreenII 62-SK plasmid to generate effectors, respectively. (c) LUC/REN activity detection verifies activation of the *BnDFR*, *BnF3H1* and *BnF3H2* promoter by BnMYB90 and BnMYB114, respectively.

Accession Numbers

The genes sequence data explained in this study are as follows: *BnMYB90* (KF738284), *BnMYB114* (XM_013835513), *BnDFR* (KF250413), *BnF3H1* (DQ288239), *BnF3H2* (NM_001316250). The protein sequences data described in this study are as follows: oilseed rape (*Brassica napus*) BnMYB90 (AIU39730) and BnMYB114 (XP_013690967); Arabidopsis (*Arabidopsis thaliana*) AtMYB21 (NP_189418), AtMYB24 (NP_198851), AtMYB114 (NP_176812), AtPAP1 (NP_176057), and AtPAP2 (NP_176813); apple (*Malusdomestica L. Borkh*) MdMYB1 (ADQ27443) and MdMYB10 (ACQ45201); tomato (*Solanumlycopersicum*) SlMYB75 (NP_001265992); potato (*Solanumtuberosum*) StMYB113 (AND01219); grape (*Vitisvinifera*) VvMYBPAP1 (NP_001268160) and VvMYBPAP2 (ACK56131); and maize (*Zea mays*) ZmC1 (AAO85386) and ZmPL (AIB04727).

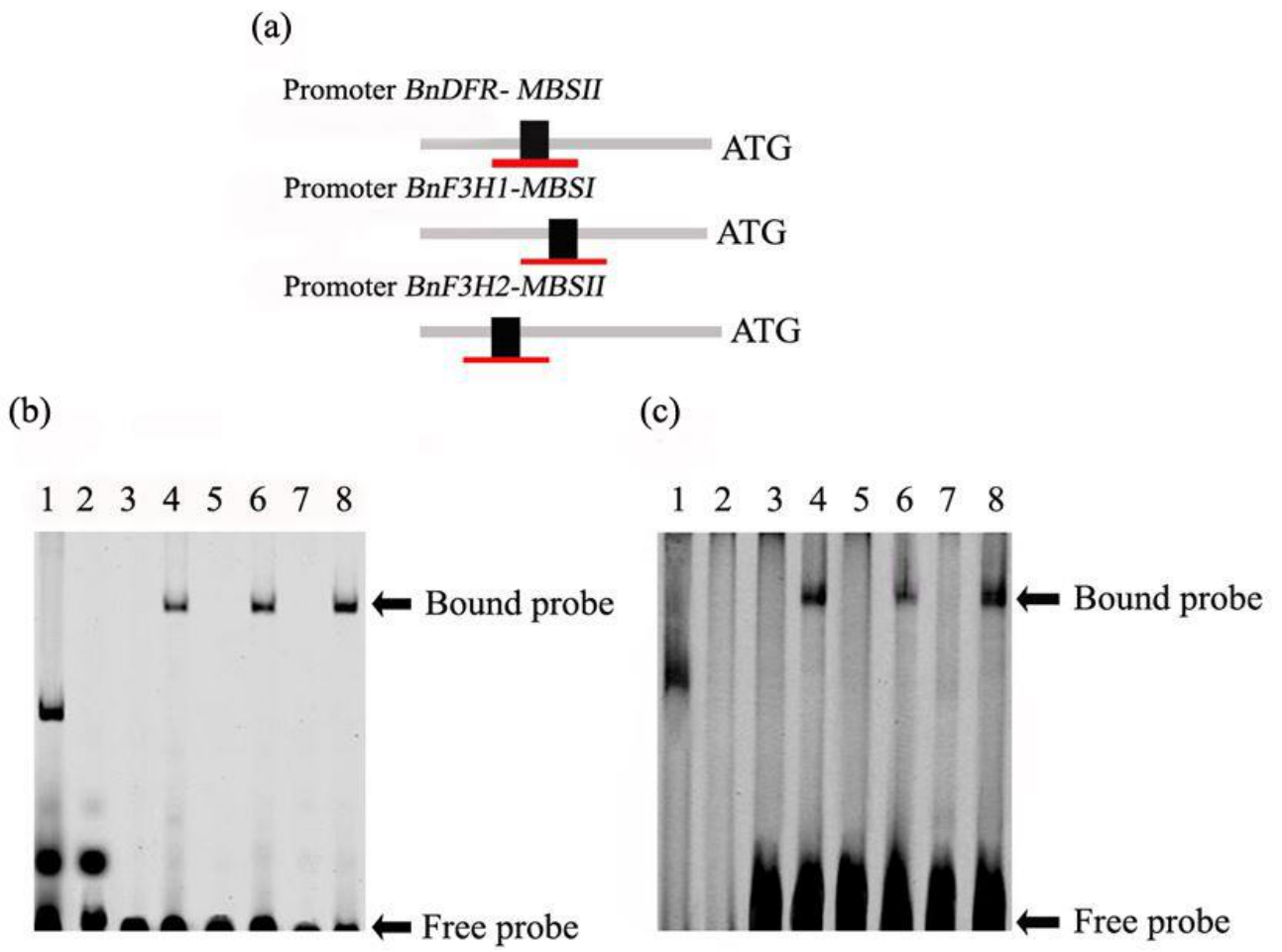

Supplemental Fig. 4. BnMYBs bind the *DFR-MBSII*, *F3H1-MBSI*, *F3H2-MBSII*. Illustrative diagram of the *BnDFR*/*BnF3H1*/*BnF3H2* promoter indicate the potential MBS. The predicted conventional sequences are showed by black boxes. (a) Red lines represent the designed probe sequences for further test. (b) Binding BnMYB90 to the *DFR-MBSII*, *F3H1-MBSI*, *F3H2-MBSII*. 1. Addition probe Gata1 as a positive control. 2. Lacking probe Gata1 as a negative control. 3, 5, 7 represent only addition *DFR-MBSII*, *F3H1-MBSI*, *F3H2-MBSII* and lacking BnMYB90-HIS. 4, 6, 8 represent *DFR-MBSII*, *F3H1-MBSI*, *F3H2-MBSII* and BnMYB90-HIS were contained in the experiment, respectively. (c) Binding BnMYB114 to the *DFR-MBSII*, *F3H1-MBSI*, *F3H2-MBSII*. 1. Addition probe Gata1 as a positive control. 2. Lacking probe Gata1 as a negative control. 3, 5, 7 represent only addition *DFR-MBSII*, *F3H1-MBSI*, *F3H2-MBSII* and lacking BnMYB114-HIS. 4, 6, 8 represent *DFR-MBSII*, *F3H1-MBSI*, *F3H2-MBSII* and BnMYB114-HIS were contained in the experiment, respectively.

Subcellular localization was an effective method for further analysis of protein function. In the present study, nucleus localizations of three genes and MYB TFs were analyzed. Clear green fluorescence of BnDFR, BnF3H1 and BnF3H2 was observed in the whole transformed cells (Fig. 3b-d). Unexpectedly, clear green fluorescence of BnMYB90 and BnMYB114 was only observed in the nucleus (Fig. 3e-f). To modulate expression of downstream genes, TFs usually locate in nucleus. Previous research indicated that AtMYB75 -yellow fluorescence was found to accumulate in the nucleus (Bhargava *et al*., 2010). Distributions of MYB TFs in other species have also been reported. Yellow fluorescence was only observed in the nucleus in transformed cells expressing *35S:YFP-EsMYB90* (Qi *et al*., 2020). When GFP-OsMYB30 and CFP-GHD7 were co-transformed into rice protoplasts, green fluorescence overlapped with cyan fluorescence, which showed that OsMYB30 was localized in the nucleus (Lv *et al*., 2017). The green fluorescence of GFP-PtrMYBs was co-localized in the nucleus along with the signals of

marker gene, indicating that PtrMYB021 and PtrMYB074 are also located in nucleus (Chen *et al*., 2019). Green fluorescence of both MYB TFs and genes were observed in the nucleus suggested that BnMYB90 and BnMYB114 may modulate directly to the target gene including *BnF3H1/2* and *BnDFR* in the nucleus.

To regulate downstream genes expression, TFs tend to bind to specific motifs in the gene upstream regions. MYB proteins bind to cis-elements with the consensus sequences TAACTG and [a(a/c)c(a/t)a(a/c)c], which are referred to as MBSI and MBSII, respectively (Nakagoshi *et al*., 1990; Urao *et al*., 1993; Ferrari *et al*., 2003). MBSI were found in the promoter sequences of *BnF3H1* and *BnF3H2*, and MBSI-like were found in the promoter sequences of*BnDFR* and *BnF3H2*. In addition, MBSII was contained in the promoter sequences of *BnDFR*/*BnF3H1*/*BnF3H2* (Supplemental Fig. 3). To demonstrate whether BnMYB90 and BnMYB114 directly bind to the promoter sequence of *BnDFR*, *BnF3H1* and *BnF3H2*, EMSAs assays were performed. These results indicated that both BnMYB90 and BnMYB114 specifically bind to the *BnDFR-II*, *BnF3H1-I* and *BnF3H2-II* (Fig. 5). In addition, as a negative control, signal HIS was shown to bind to *BnDFR-II*, *BnF3H1-I* and *BnF3H2-II*, which suggested that the internal protein of HIS bacterial fluid weakly bind to the motif in the promoter of the three genes mentioned above (Supplemental Fig. 4). To verify whether BnMYB90 and BnMYB114 directly bind to the promoter sequence of *BnDFR*, *BnF3H1* and *BnF3H2 In vivo*, transient dual luciferase assays were done, which indicated that both BnMYB90 and BnMYB114 specifically bind to the *BnDFR-II*, *BnF3H1-I* and *BnF3H2-II* in *N. benthamiana* leaves (Fig. 6). Previous research indicated that AtMYB1 specifically bound to MBSI, and the bond disappeared when the MYB binding site (TAACTG) included two point mutations (TCCCTG) (Nakagoshi *et al*., 1990; Urao *et al*., 1993). In the present research, we also verified the specific bond disappeared when the MBSI included three point mutations (Figs. 5 and 6). In addition, previous research indicated the promoter regions of *AtPGIP1* and *AtPGIP2* contained the MBSII binding site (Ferrari *et al*., 2003). Our experimental results also showed the specific binding disappeared when MBS II included two point mutations (Figs. 5 and 6). In the study, the present EMSA assays and transient dual luciferase assays *In vivo* suggested that with the exception of reported conserved sites in MBSI and MBSII, other conserved sites found in MBSI and MBSII, are also important to MYB TFs specific binding and to MYB function in anthocyanin accumulation in oilseed rape. In the future, transformation of different TFs into oilseed rape needs to be performed in order to study single transcription factor or transcription factor complexes that result in the alteration of anthocyanin accumulation in *Brassica napus*.

Conclusions

In summary, both *BnMYB90* and *BnMYB114* are homology genes of AtPAP1 and AtPAP2 in Arabidopsis. Transcription level of BnMYB90 and BnMYB114 are detected in various tissues. The BnMYB90-eGFP and BnMYB114-eGFP accumulated at the nucleus of onion epidermal cells thereby regulate gene expression as transcription factor. BnMYB90 and BnMYB114 bind to promoter region of BnDFR and BnF3H were verified by yeast one-hybrid assay. Furthermore, the binding is verified specific by EMSA. At the same time, the binding is demonstrated *In vivo* by Transient dual luciferase assay. Taken together, our presents experiment results provide a preliminary mechanism of how MYB TFs influence anthocyanin synthesis in oilseed rape.

Acknowledgements

We are very thankful to Professor YujinHao (Shandong Agricultural University) for providing Dual Luciferase assay vectors. We thank Professor Peng Qin (Sichuan Agricultural University) for providing the PET-28a (+) vector. And we thank Professor Chaowen Xiao (Sichuan University) to help analysis promoter motif. The seed in the study was provided by the Oilseed Rape Research Center at Sichuan Agricultural University. The work was funded by the applied basic research project in Sichuan province of China (2018JY0212).

References

Aida, M., D. Beis, R. Heidstra, V. Willemsen, I. Blilou, C. Galinha, L. Nussaume, Y.S. Noh, R. Amasino and B. Scheres. 2004. The PLETHORA genes mediate patterning of the Arabidopsis root stem cell niche. *Cell*., 119: 109-120.

Albert, N.W., K.M. Davies, D.H. Lewis, H. Zhang, M. Montefiori, C. Brendolise, M.R. Boase, H. Ngo, P.E. Jameson and K.E. Schwinn. 2014. A conserved network of transcriptional activators and repressors regulates anthocyanin pigmentation in Eudicots. *Plant Cell*., 26: 962-980.

An, J.P., X.F. Wang, Y.Y. Li, L.Q. Song, L.L. Zhao, C.X. You and Y.J. Hao. 2018. EIN3-LIKE1, MYB1, and ETHYLENE RESPONSE FACTOR3 act in a regulatory loop that synergistically modulates ethylene biosynthesis and anthocyanin accumulation. *Plant Physiol*., 178: 808-823.

An, X.H., Y. Tian, K.Q. Chen, X.J. Liu, D.D. Liu, X.B. Xie, C.G. Cheng, P.H. Cong and Y.J. Hao. 2015. MdMYB9 and MdMYB11 are involved in the regulation of the JA-induced biosynthesis of anthocyanin and proanthocyanidin in apples. *Plant Cell and Physiol*., 56: 650-662.

Andreu, V., B. Lagunas, R. Collados, R. Picorel and M. Alfonso. 2010. The GmFAD7 gene family from soybean: identification of novel genes and tissue-specific conformations of the FAD7 enzyme involved in desaturase activity. *J. Exp. Bot*., 61: 3371-3384.

Banilas, G., A. Moressis, N. Nikiloudakis and P. Hataopous. 2005. Spatial and temporal expression of two distincoleatedesaturases from olive (*Olea europaea* L.). *Plant Sci*., 168: 547-555.

Beaudoin, F., X. Wu, F. Li, R.P. Haslam, J.E. Markham, H. Zheng, J.A. Napier and L. Kunst. 2009. Functional characterization of the Arabidopsis beta-ketoacyl-coenzyme A reductase candidates of the fatty acid elongase. *Plant Physiol*., 150: 1174-1191.

Bhargava, A., S.D. Mansfield, H.C. Hall, C.J. Douglas and B.E. Ellis. 2010. MYB75 functions in regulation of secondary cell wall formation in the Arabidopsis inflorescence stem. *Plant Physiol*., 154: 1428-1438.

Borevitz, J.O., Y.J. Xia, J. Blount, R.A. Dixon and C. Lamb. 2000. Activation tagging identifies a conserved MYB regulator of phenylpropanoid biosynthesis. *Plant Cell*., 12: 2383-2394.

Chagne, D., K.L. Wang, R.V. Espley, R.K. Volz, N.M. How, S. Rouse, C. Brendolise, C.M. Carlisle, S. Kumar, N.D. Silva, D. Micheletti, T. McGhie, R.N. Crowhurst, R.D. Storey, R. Velasco, R.P. Hellens, S.E. Gardiner and A.C. Allan. 2013. An ancient duplication of apple MYB transcription factors is responsible for novel red fruit-flesh phenotypes. *Plant Physiol*., 161: 225-239.

Chen, H., J.P. Wang, H.Z. Liu, H.Y. Li, Y.J. Lin, R. Shi, C.M. Yang, J.H. Gao, C.G. Zhou, Q.Z. Li, R.R. Sederoff, W. Liand V.L. Chiang. 2019. Hierarchical transcription factor and chromatin binding network for wood formation in Populustrichocarpa. *Plant Cell*., 31: 602-626.

Cone, K.C., F.A. Burr and B. Burr. 1986. Molecular analysis of the maize anthocyanin regulatory locus C1. *P Natl. Acad. Sci. USA*., 83: 9631-9635.

Espley, R.V., R.P. Hellens, J. Putterill, D.E. Stevenson, S. Kutty-Amma and A.C. Allan. 2007. Red colouration in apple fruit is due to the activity of the MYB transcription factor, MdMYB10. *Plant J*., 49: 414-427.

Ferrari, S., D. Vairo, F.M. Ausubel, F. Cervone and G.D. Lorenzo. 2003. Tandemly duplicated Arabidopsis genes that encode polygalacturonase-inhibiting proteins are regulated coordinately by different signal transduction pathways in response to fungal infection. *Plant Cell*., 15: 93-106.

Francisco, R.M., A. Regalado, A. Ageorges, B.J. Buela, B. Bassin, C. Eisenach, O. Zarrouk, S. Vialet, T. Marlin, M.M. Chaves, E. Martinoia and R. Nagy. 2013. ABCC1, an ATP binding cassette protein from grape berry, transports anthocyanidin 3-*O*-Glucosides. *Plant Cell*., 25: 1840-1854.

Fu, W.Q., D.Z. Chen, Q. Pan, F.F. Li, Z.G. Zhao, X.H. Ge and Z.Y. Li. 2018. Production of red-flowered oilseed rape via the ectopic expression of *Orychophragmus violaceus* OvPAP2.*Plant Biotechnol J*., 16: 367-380.

Galinha, C., H. Hofhuis, M. Luijten, V. Willemsen, I. Blilou, R. Heidstra and B. Scheres. 2007. PLETHORA proteins as dose-dependent master regulators of Arabidopsis root development. *Nature*, 449: 1053-1057.

Golawska, S., I. Sprawka, I. Lukasik and A. Golawski. 2014. Are naringenin and quercetin useful chemicals in pest-management strategies? *J. Pest. Sci*., 87: 173-180.

Gonzalez, A., M. Zhao and J.A. Leavitt. 2010. Regulation of the anthocyanin biosynthetic pathway by the TTG1/bHLH/ MYB transcriptional complex in Arabidopsis seedlings. *Plant J*., 53: 814-827.

Gould, K.S. 2004. Nature's swiss army knife: The diverse protective roles of anthocyanins in leaves. *J Biomed Biotechnol*., 2004: 314-320.

Grotewold, E., P. Athma and T. Peterson. 1991. Alternatively spliced products of the maize P gene encode proteins with homology to the DNA-binding domain of myb-like transcription factors. *P NatlAcadSci USA*., 88: 4587-4591.

Harborne, J.B. and C.A. Williams. 2000. Advances in flavonoid research since 1992. *Phytochemistry*, 55: 481-504.

Hatzopoulos, P., G. Banilas, K. Giannoulia, F. Gazis, N. Nikoloudakis, D. Milioni and K. Haralampidis. 2002. Breeding, molecular markers and molecular biology of the olive tree. *Eur. J. Lipid. Sci. Tech*., 104: 547-586.

Holton, T.A. and E.C. Cornish. 1995. Genetics and biochemistry of anthocyanin biosynthesis. *Plant Cell*., 7: 1071-1083.

Jaakola, L. 2013. New insights into the regulation of anthocyanin biosynthesis in fruits.*Trends in Plant Sci*., 18: 447-483.

Jin, W.M., H. Wang, M.F. Li, J. Wang, Y. Yang, X. Zhang, G. Yan, H. Zhang, J.S. Liu and K.C. Zhang. 2016. The R2R3 MYB transcription factor PavMYB10.1 involves in anthocyanin biosynthesis and determines fruit skin in sweet cherry (*Prunu savium* L.). *Plant Biotechnol. J*., 14: 2120-2133.

Joubes, J., S. Raffaele, B. Bourdenx, C. Garcia, J. Laroche-Traineau, P. Moreau, F. Domergue and R. Lessire. 2008. The VLCFA elongase gene family in *Arabidopsis thaliana*: phylogenetic analysis, 3D modeling and expression profiling. *Plant Mol. Biol*., 67: 547-566.

Kim, H.U., Y.B. Li and A.H. Huang. 2005. Ubiquitous and endoplasmic reticulum-located lysophosphatidyl acyltransferase, LPAT2, is essential for female but not male gametophyte development in Arabidopsis. *Plant Cell*., 17: 1073-1089.

Kobayashi, S., N. Goto-Yamamoto and H. Hirochika. 2004. Retrotransposon-induced mutations in grape skin color. *Science*, 304: 982.

Li, C.J., L. Shi, Y.N. Wang, W. Li, B.Q. Chen, L. Zhu and Y. Fu. 2019. Arabidopsis ECAP is a new adapter protein that connects JAZ repressors with the TPR2 Corepressor to suppress jasmonate responsive anthicyanin accumulation. *Mol. Plant*., 13: 246-265.

Li, Y.Y., K. Mao, C. Zhao, X.Y. Zhao, H.L. Zhang, H.R. Shu and Y.J. Hao. 2012. MdCOP1 ubiquitin E3 ligases interact with MdMYB1 to regulate light-induced anthocyanin biosynthesis and red fruit coloration in apple. *Plant Physiol*., 160: 1011-1022.

Liu, C.Y., J. Tang and L.Y. Zhao. 2018. Research progress on the stability and function of anthocyanins. *Hans J. Food Nutrition Sci*., 7: 53-63.

Liu, K., G. Xiao, Z.Q. Zhang, C.Y. Guan, S.Y. Chen and X.M. Wu. 2016. Expression of five genes related to fatty acid metabolism in different growth stages of rape. *BMC Biol*., 33: 32-34.

Loreti, E., G. Povero, G. Novi, C. Solfanelli, A. Alpi and P. Perata. 2008. Gibberellins, jasmonate and abscisic acid modulate the sucrose-induced expression of anthocyanin biosynthetic genes in Arabidopsis. *New Phytol*., 179: 1004-1016.

Lv, Y., M. Yang, D. Hu, Z.Y. Yang, S.Q. Ma, X.H. Li and L.Z. Xiong. 2017. The OsMYB30 transcription factor suppresses cold tolerance by interacting with a JAZ protein and suppressing β-amylase expression. *Plant Physiol*., 173: 1475-1491.

Mathews, H., S.K. Clendennen., C.G. Caldwell, X.L. Liu, K. Connors, N. Matheis, D.K. Schuster, D.J. Menasco, W. Wagoner, J. Lightner and D.R. Wagner. 2003. Activation tagging in tomato identifies a transcriptional regulator of anthocyanin biosynthesis, modification, and transport. *Plant Cell*., 15: 1689-1703.

Mellway, R.D., L.T. Tran, M.B. Prouse, M.M. Campbell and C.P. Constabel. 2009. The wound-, pathogen-, and ultraviolet B-responsive MYB134 gene encodes an R2R3 MYB transcription factor that regulates proanthocyanidin synthesis in Poplar. *Plant Physiol*., 150: 924-941.

Miller, J.F., D.C. Zimmerman and B.A. Vick. 1987. Genetic control of high oleic acid content in sunflower oil. *Crop Sci*., 27: 923-926.

Montefiori, M., C. Brendolise, A.P. Dare, K. Lin-Wang, K.M. Davies, R.P. Hellens and A.C. Allan. 2015. In the Solanaceae, a hierarchy of bHLHs confer distinct target specificity to the anthocyanin regulatory complex. *J. Exp. Bot*., 66: 1427-1436.

Nakagoshi, H., T. Nagase, C. Kanei-lshii, Y. Ueno and S. Lshii. 1990. Bing of the c-myb proto-oncogene product to the simian virus 40 enhancer stimulates transcription. *J. Biol. Chem*., 265: 3479-3483.

Nishizaki, Y., M. Yasunaga, E. Okamoto, M. Okamoto, Y. Hirose, M. Yamaguchi, Y. Ozeki and N. Sasaki. 2013. *p*-hydroxybenzoyl-glucose is a zwitter donor for the biosynthesis of 7-polyacylated anthocyanin in delphinium. *Plant cell*., 25: 4150-4165.

Owens, D.K. and C.A. Mclntosh. 2011. Biosynthesis and function of citrus glycosylated flavonoids. In: *The Biological Activity of Phytochemicals*. (Eds.): David, R. Springer, New York, pp. 67-95.

Paz-Ares, J. 1987. The regulatory C1 locus of *Zea mays* encodes a protein with homology to myb proto-oncogene products and with structural similarities to transcriptional activators. *EMBO J*., 6: 3553-3558.

Peters, D.J. and C.P. Constabel. 2002. Molecular analysis of herbivore-induced condensed tannin synthesis: cloning and expression of dihydroflavonolreductase from trembling aspen (*Populus tremuloides*). *Plant J*., 32: 701-712.

Qi, T.C., S.S. Song, Q.C. Ren, D.W. Wu, H. Huang, Y. Chen, M. Fan, W. Peng, C.M. Ren and D.X. Xie. 2011. The Jasmonate-ZIM-Domain proteins interact with the WD-Repeat/bHLH/MYB complexes to regulate jasmonate-mediated anthocyanin accumulation and trichome initiation in Arabidopsis thaliana. *Plant Cell*., 23: 1795-1814.

Qi, Y.T., C.H. Gu, X.J. Wang, S.Q. Gao, C.S. Li, C.Z. Zhao, C.S. Li, C.L. Ma and Q. Zhang. 2020. Identification of the eutremasalsugineum EsMYB90 gene important for anthocyanin biosynthesis. *BMC Plant Biol*., 20: 186.

Quattrocchio, F., W. Verweij, A. Kroon, C. Spelt, J. Moland R. Koes. 2006. PH4 of petunia is an R2R3 MYB protein that activates vacuolar acidification through interactions with basic-helix–loop–helix transcription factors of the anthocyanin pathway. *Plant Cell*., 18: 1274-1291.

Roscoe, T.J. 2005. Identification of acyltransferases controlling triacylglycerol biosynthesis in oilseeds using a genomics-based approach. *Eur. J. Lipid. Sci. Tech*., 107: 256-262.

Salazar-Henao, J., R. Lehner, I. Betegon-Putze, J. Vilarrasa-Blasi and A.I. Cano-Delgado. 2016. BES1 regulates the localization of the brassinosteroid receptor BRL3 within the provascular tissue of the Arabidopsis primary root. *J. Exp. Bot*., 67: 4951-4961.

Shimada, T., Y. Wakita, M. Otani and K. Iba. 2010. Modification of fatty acid composition in rice plants by transformation with a tobacco microsomal ω-3 fatty acid desaturase gene (NtFAD3). *Plant Cell Tiss. Org*., 17: 43-48.

Snowden, K.C., A.J. Simkin, B.J. Janssen, K.R. Templeton, H.M. Loucas, J.L. Simons, S. Karunairetnam, A.P. Gleave, D.G. Clark and H.J. Klee. 2005. The decreased apical dominance1/petunia hybrida CAROTENOID CLEAVAGE DIOXYGENASE8 gene affects branch production and plays a role in leaf senescence, root growth, and flower development. *Plant Cell*., 17: 746-759.

Solovchenko, A. and M. Schmitz-Eiberger. 2003. Significance of skin flavonoids for UV-B-protection in apple fruits. *J Exp. Bot*., 54: 1977-1984.

Stracke, R., M. Werber and B. Weisshaar. 2001. The R2R3-MYB gene family in Arabidopsis thaliana.*CurrOpin Plant Biol*., 4: 447-456.

Sun, C.L., L. Deng, M.M. Du, J.H. Zhao, Q. Chen, T.T. Huang, H.L. Jiang, C.B. Li and C.Y. Li. 2020. A transcriptional network promotes anthocyanin biosynthesis in tomato flesh. *Mol. Plant*, 13: 42-58.

Tao, R.Y., W.J. Yu, Y.H. Gao, J.B. Ni, L. Yin, X. Zhang, H.X. Li, D.S. Wang, S.L. Bai and Y.W. Teng. 2020. Light-induced basic/helix-loop-helix64 enhances anthocyanin biosynthesis and undergoes Constitutively Photomorphogenic1-mediated degradation in Pear. *Plant Physiol*., 184: 1684-1701.

Teng, S., J. Keurentjes, L. Bentsink, M. Koornneef and S. Smeekens. 2005. Sucrose-specific induction of anthocyanin biosynthesis in Arabidopsis requires the MYB75/PAP1 gene. *Plant Physiol*., 139: 1840-1852.

Urao, T., K.Y. Shinozaki, S. Urao and K. Shinozaki. 1993. An Arabidopsis myb homolog is induced by dehydration stress and its gene product binds to the conserved MYB recognition sequence. *Plant Cell*, 5: 1529-1539.

Wang, L.H., W. Tang, Y.W. Hu, Y.B. Zhang, J.Q. Sun, X.H. Guo, H. Lu, Y. Yang, C.B. Fang, X.L. Niu, J.Y. Yue, Z.J. Fei and Y.S. Liu. 2019. A MYB/bHLH complex regulates tissue-specific anthocyanin biosynthesis in the inner pericarp of red-centered kiwifruit Actinidiachinensis cv. Hongyang. *Plant J*., 99: 359-378.

Wickramarathna, D., M. Siloto, E. Mietkiewska, D. Singer, X. Pan and R.J. Weselake. 2015. Heterologous expression of flax Phospholipid: Diacylglycerol cholinephosphotransferase (PDCT) increases polyunsaturated fatty acid content in yeast and Arabidopsis seeds. *BMC Biotechnol*., 15: 63.

Xiao, S., L.Y. Dai, F.Q. Liu, Z.L. Wang, W. Peng and D.X. Xie. 2004. COS1: an Arabidopsis coronatine insensitive1 suppressor essential for regulation of jasmonate-mediated plant defence and senescence, *Plant Cell*., 16: 1132-1142.

Xie, X.B., S. Li, R.F. Zhang, J. Zhao, Y.C. Chen, Q. Zhao, Y.X. Yao, C.X. You, X.S. Zhang and Y.J. Hao. 2012. The bHLHreanscription factor MdbHLH3 promotes anthocyanin accumulation and fruit colouration in response to low temperature in apples. *Plant Cell Environ*., 35: 1884-1897.

Xu, W.J., C. Dubos and L. Lepiniec. 2015. Transcriptional control of flavonoid biosynthesis by MYB-bHLH-WDR complexes. *Trends in Plant Sci*., 20: 176-185.

Yao, Y.M., K.X. Li, H.D. Liu, R.W. Duncan, S.M. Guo, L. Xiao and D.Z. Du. 2017. Whole-genome re-sequencing and fine mapping of an orange petal color gene (Bnpc1) in spring *Brassica napus* L to 1 151-kb region. *Euphytica*., 213: 165.

Yoshida, Y., R. Sano, T. Wada, J. Takabayashi and K. Okada. 2009. Jasmonic acid control of GLABRA3 links inducible defence and trichome patterning in Arabidopsis. *Development*, 136: 1039-1048.

Zhou, Y., H. Zhou, K.L. Wang, S. Vimolmangkang, V. Espley, L. Wang, A.C. Allan and Y.P. Han 2014 Transcriptome analysis and transient transformation suggest an ancient duplicated MYB transcription factor as a candidate gene for leaf red coloration in peach. *BMC Plant Biol*., 14: 388-400.

Zimmermann, I.M., M.A. Heim, B. Weisshaar and J.F. Uhrig. 2004. Comprehensive identification of *Arabidopsis thaliana* MYB transcription factors interacting with R/B-like bHLH proteins. *Plant J*., 40: 22-34.

Zuluaga, D.L., S. Gonzali, E. Loreti, C. Pucciariello, E. Degl'lnnocenti, L. Guidi, A. Alpi and P. Perata. 2008. *Arabidopsis thaliana* MYB75/PAP1 transcription factor induces anthocyanin production in transgenic tomato plants. *Functional Plant Biol*., 35: 606-618.

(Received for publication 10 May 2020)